Maaß et al. 2011, Analysis of particle strain in stirred bioreactors by drop breakage investigations, accepted article, Biotechnol. J., DOI: 10.1002/biot.201100161

ANALYSIS OF PARTICLE STRAIN IN STIRRED BIOREACTORS BY DROP BREAKAGE INVESTIGATIONS

Sebastian Maaß[1*], Susanne Buscher[1], Stephanie Hermann[1] and Matthias Kraume[1]

[1]Technische Universität Berlin, Straße des 17. Juni 135, Sekr. MA 5-7, 10623 Berlin, Germany

[*]corresponding author (sebastian.maass@tu-berlin.de)

ABSTRACT

Understanding of particle strain and drop breakage is relevant for various technical applications. To analyze it single drop experiments in a breakage cell and evolving drop size distributions in an agitated system are studied. The mechanisms for particle strain and drop breakage are assumed to be comparable for the investigated turbulent flow regime. The agitation process is simulated using a population balance model. This model provides transient prediction capacities at different scales and therefore, can be used for scale-up/down projects.

The single drop experiments provide necessary information, which are needed within the population balance equations. The number and the size distributions of daughter fragments for single drops have been studied. The results clearly support the assumption of binary breakage. The most common assumption of a Gaussian distribution for the daughter drop size distribution could not be supported.

The evolution of a breakage dominated toluene/water system was than simulated using different daughter drop size distributions from literature. The computational results were compared with experimental values. All simulations were able to predict the transient Sauter mean diameter excellent but varied strongly in the results on the shape of the distribution. In agreements to the experimental single drop results the use of a bimodal or a very broad bell-shaped distribution of the daughter drops is proposed for the simulations.

Although these results were obtained in a particular vessel for a specific phase system it can be applied to simulate transient multiphase systems at different scales. We would expect that the general trends observed in this study are comparable to various applications in multiphase bioreactors.

KEYWORDS:

Drop breakage, particle strain, population balance equation, liquid-liquid dispersion, daughter drops size distribution, number of daughter drops

1 INTRODUCTION

Stirred reactors play a major role in biotechnology, the pharmaceutical and chemical industry. For the evaluation of such reactors regarding quality, economy and also environmental aspects, the occurring particle strain is very important, as actual research shows [1].

Concerning biotechnology and pharmaceutical processes the following examples should clarify the meaning and importance of the particle strain: agitated fermentation processes using eukaryotic cells without protecting cell walls are restricted due to the rotating stirrer and the thereby caused turbulent flow conditions which lead to the destruction of the cells. It is also well known that mechanical stress leads to decreased activities of enzymes in stirred reactors or bubble column reactors [2, 3]. Also for plant cell cultures with cell walls the productivity is restricted due to the stirring conditions, although the cells are not destroyed by the stirring process [4].

Many fermentation processes are carried out in mechanically agitated bioreactors containing two or more phases. Also a range of these processes exist in which the carbon source is in the form of a water-immiscible oil phase. Therefore, these constitute of three-phases. Furthermore, oils have been widely adopted in antibiotic production and their utilization in industrial fermentations. They, in addition to being the main or a supplementary carbon source, have been claimed to protect fragile mutants and also to reduce the concentration in the media of some inhibitory metabolites, including the antibiotics themselves, by virtue of their high solubility in the oil. Also, the use of oils has obvious advantages in the production of lipid soluble materials (e.g., beta-carotene). Furthermore, the use of oils is beneficial in improving the yields of a variety of fermentations, such as those for the production of riboflavin and citric [5]. Many of the aforementioned examples are extractive fermentations. Maintenance of interfacial area is one of the key requirements for successful and reproducible scale-up for biotransformation processes [6]

The physical understanding and mathematical description of particle strain and drop breakage in stirred systems is therefore of very high interest. This work focuses on the analysis of particle strain in stirred liquid/liquid-systems under turbulent conditions. The drop size distributions are thereby determined by drop breakage and drop coalescence processes. To get a deeper insight and improve the physical understanding, both phenomena should be investigated independently from each other. In this work the drop breakage, basically caused by the fluid dynamic stress of the continuous flow, is investigated.

The goal of the work is to provide a model approach for turbulent multiphase systems, occurring in bioreactors, describing the drop size over time as a function of process parameters and reactor geometry.

A detailed description of dispersed phase characteristics can be obtained by using the population balance equation (PBE) that was introduced in the mid-1960s to simulate particulate processes. PBE have since become a well established tool that is widely used for simulating multi phase operations because it has the advantage of being able to describe particulate processes in terms of identifiable physical parameters (size, concentration, age) and operational conditions (power input, temperature, pressure, reactor volume) [7]. For a mathematical description the submodels from literature have to be validated and if needed improved.

An overview of and a short introduction into population balance models is given in chapter two. The used experimental and numerical methods to investigate particle strain based on breakage dominated liquid-liquid systems are given in chapter three. The number and the size

distribution of daughter drops are determined experimentally in this work. These results based on single drop experiments build the first part of the results section. In the second part the transient drop size distribution in a stirred vessel is investigated experimentally and compared with PBE simulations using different models for the daughter drop size distribution. The concluding remarks propose a PBE model combination for agitated vessel, which is useable for process analysis, reactor design, scale-up and optimization.

2 POPULATION BALANCE EQUATION

PBE describe the temporal variation in dispersed phase characteristics where the dispersed phase is considered as an assembly of particles or cells whose individual identities are being continually changed over time. Therefore, the PBE belong to a subcategory of equations known as partial differential equations. As no heat or mass transfer, particle growth or chemical reaction took place in this study and all experiments were carried out for liquid/liquid dispersion under batch conditions, the connected PBE can be expressed as a univariate PBE, which only considers size change of the individuals:

$$\frac{\partial f(V_p)}{\partial t} = B_b(V_P,t) - D_b(V_P,t) + B_c(V_P,t) - D_c(V_P,t) \tag{1}$$

Here B_b, D_b, B_c and D_c are the birth rate by breakage, death rate by breakage, birth rate by coalescence, and death rate by coalescence, respectively. While the coalescence efficiency is assumed to be zero in this work the birth and death term by breakage are described as follows:

$$\frac{\partial f(V_p)}{\partial t} = \int_{V_p}^{V_{P,max}} \nu(V_p')\beta(V_p,V_p')g(V_p')f(V_p',t)dV_P - g(V_p)f(V_p,t) \tag{2}$$

where $g(V_P)$ is the breakage frequency, $\nu(V_P)$ is the number of dispersed fluid entities formed upon breakage of a particle V_P, and $\beta(V_P,V_P')$ is the size distribution of daughter fragments formed from the breakage of a particle V_P.

A profound overview of existing model approaches for the breakage rate is given by Liao and Lucas [8]. In many cases the authors assume that drop breakage occurs due to drop-eddy collisions. The most widely used and quoted model for the drop breakage rate is the approach of Coulaloglou and Tavlarides [9] given in equation (3).

$$g(d_p) = c_{1,b}\frac{\varepsilon^{1/3}}{(1+\varphi_d)d_P^{2/3}}\exp\left(-c_{2,b}\frac{\gamma(1+\varphi_d)^2}{\rho\varepsilon^{2/3}d_P^{5/3}}\right) \tag{3}$$

In combination with the breakage rate, the number of daughter drops ν and the daughter drop size distribution $\beta(d_p,d_p')$ have to be formulated.

2.1 Number of daughter drops

The most used assumption in PBE modeling is that one mother drop breaks into two daughter drops (therefore ν is equal to 2) with a maximum probability of forming two equal sized daughter drops. This is based on some few experimental results, although opposing results have been reported. These literature data will be briefly discussed here as it provides a base

for the comparison with own single drop experiment results, which will be discussed in the results section.

Konno et al. [10] used high-speed photography to directly observe drop breakage events in stirred vessels. To avoid coalescence they always used a dilute liquid/liquid system with a dispersed phase fraction lower than 0.2 %. The breakage time, drop path and the number of drops per breakage event were recorded. The investigated mother drop sizes were in the range of 0.26 – 1.0 mm. Konno et al. [10] determined the mean number of daughter drops between 2.6 – 4.4. The major drawback of their approach is the insufficient number of breakage events for statistically meaningful results. For a strong varying mother drop diameter they measured less than a hundred breakage events.

Hesketh et al. [11] studied both, drop and bubble breakup. They reported that only binary breakup occurred in the turbulent pipe flow they studied. Their number of observed drop breakage events is very low. The twelve events measured do not allow a statistically confident interpretation. However, they observed that unequal-sized breakup was the result of all drop breakages mainly caused by elongation.

Bahmanyar and Slater [12] determined minimum energy dissipation rates at which drops of a given size do not break. The mean number of daughter drops produced by breakage was correlated as a simple function of the drop diameter based on the critical diameter and agreement was found with data from other types of agitated systems. Based on the works of Hancil and Rod [13] they correlated their number of daughter drops as follows:

$$\nu = 2 + 0.9\left[\left(d_P / d_{P,crit}\right) - 1\right] \tag{4}$$

Starting at binary breakage the number of particles is increasing with increasing mother drop diameter d_P. Due to the low time resolution of their measurement techniques (capillary and video technique) they were not able to determine the number of daughter drops connected to a single breakage event. Kuriyama et al. [14] investigated single drop breakage events in a stirred vessel, which were induced via a loop flow into the stirrer zone. They analyzed the dependency of different high viscosities (0.1 – 12.6 Pa·s) of the dispersed phase on the number of daughter drops. The continuous phase was always pure water. Generally, they observed a dependency of the number of daughter drops on the mother drop diameter. A direct proportionality was found over the whole viscosity range by using a viscosity correction term:

$$\nu \propto \sqrt{\frac{\eta_d}{\eta_c}} \cdot d_P^{\,0.455} \tag{5}$$

The studies by Eastwood et al. [15] were dealing with drop breakage in a turbulent liquid jet. They found that drops were considerably elongated before breakage. The deformation or stretching rose with increasing drop viscosity. The stretching occurred on scales comparable to the turbulent integral length scale, and some deformed drops seemed to rotate with the flow structures. The authors propose that the elongated particle break is caused by capillary effects resulting from differences in the radius of curvature along their length. Therefore, they scale the breakage time with the capillary time and draw similarities to laminar breakage. It was

difficult for them to identify the number of fragments quantitatively but they stated that multiple breakup is most probable for their investigated system. Galinat et al. [16] quantified this statement in a pipe flow for heptane drops by swarm and single drop experiments. They investigated the number of daughter drops and the resulting daughter drop size distribution as a function of the flow velocity and mother drop diameter. The increase of both influence parameters lead to a strong increase of the number of daughter drops.

Andersson and Andersson [17] investigated the dynamics of bubble and drop breakage with a high-speed technique. The interpretation of the work by Anderson and Anderson [17] is difficult, while neither definition for their analyzed breakage events nor the overall amount of investigated events is given by the authors. However, their qualitative investigations propose binary breakage for bubbles but multiple break-up for drops. The number of daughter drops for their investigated dodecane/water system was decreasing with increasing energy dissipation. The absolute value for an average ν of this system was given of around 3.2. A summary for the different results in the different references on the number of daughter drops is given in Table 1.

Table 1 – Experimental results in literature for the number of daughter drops

Reference	experimental set-up	used frame rate [fps]	number of daughter drops ν [-]
Konno et al. [10]	stirred vessel	4000	2.6 – 4.4
Hancil and Rod [13]	stirred vessel	n/a	2.4 – 6
Kuriyama et al. [14]	loop reactor/ stirred vessel	n/a	4 – 27
Galinat et al. [16]	orifice flow	456	2 – 8
Anderson and Anderson [17]	static mixed reactor	1000	3.2

2.2 Daughter drop size distribution

According to Liao and Lucas [8] daughter drop size distributions (DDSD) can be statistical or phenomenological approaches. As to pure statistical models, daughter drop sizes are invariant to the properties of the dispersed phase, the mother drop diameter or power input. That is not true for phenomenological daughter drop size distributions. Liao and Lucas [8] also distinguished the distributions regarding their shapes: Bell-shaped distributions assume a maximum probability density for daughter drops of equal size. Contrarily, U-shaped and M-shaped distributions predict a minimum probability density for the same event. However, bell-shaped and M-shaped distributions have in common a zero probability density for infinitively small daughter drops, while U-shaped distributions predict these daughter drops most probable.

2.2.1 Statistical daughter drop size distributions

The most widely used daughter drop size distribution is the Gaussian distribution, as done by Coulaloglou and Tavlarides [9]. The expectation value is $\mu = V_P/\nu$ with $\nu = 2$, if a maximum probability density for equal sized daughter drops is postulated. The standard deviation is expressed as $\sigma = \mu/c$, assuming that $c = 2.5$. The dimensionless representation is given with the daughter to mother drop volume ratio $f = V'_P/V_P$ as follows:

$$\beta(f,1) = \frac{c\nu}{\sqrt{2\pi}} \exp\left(-\frac{(\nu f - 1)^2 c^2}{2}\right) \tag{6}$$

Another statistical approach often referred to is the beta distribution. The dimensionless representation is given as follows:

$$\beta(f,1) = \frac{\Gamma(a+b)}{\Gamma(a)\Gamma(b)} f^{a-1}(1-f)^{b-1} \tag{7}$$

To yield a symmetrical distribution over f, which is necessary for binary breakage (see Ramkrishna [18]), the parameters a and b must be equal. Following Lee et al. [19], they are set as $a = b = 2$.

Both the Gaussian and the beta distribution are bell-shaped. However, if it is supposed that daughter drops of different sizes are most probable an asymmetric statistical distribution can be used. Note, that it has to be mirrored at $f = 0.5$ to meet the symmetry condition. Furthermore, this mirrored distribution must be divided by its integral over the volume ratio f in order to be normalized and mass conserving (see Ramkrishna [18]).

In the present paper, a mirrored Gaussian distribution is used as another statistical approach. This idea was introduced by Kostoglou et al. [20] and it reflects the experimental results, discussed later, which show an M- and U-shaped distribution. The expectation value is set to $1/6 \cdot V_P$ and $5/6 \cdot V_P$, respectively. Because the integral of a Gaussian distribution is 1 and the distribution is mirrored at $f = 0.5$, the function has to be divided by 2. The dimensionless representation is given as follows:

$$\beta(f,1) = \begin{cases} \frac{15}{\sqrt{2\pi}} \exp\left(-\frac{25}{8}(6 \cdot f - 1)^2\right) & ; \quad \text{for } f \le 0.5 \\ \beta(1-f,1) & ; \quad \text{for } f > 0.5 \end{cases} \tag{8}$$

This mirrored Gaussian distribution is M-shaped and equals zero for equal sized daughter drops. The maximum probability density is reached at $f = 1/6$ and $f = 5/6$, respectively.

2.2.2 The daughter drop size distribution of Tsouris and Tavlarides

The phenomenological model of Tsouris and Tavlarides [21] postulates that the increase of the interfacial energy appears as a consequence of the drop breakage which governs the eventual daughter drop sizes. The additional interfacial energy demand is proportional to the increase of the interface as follows:

$$\Delta E \quad \sim \quad -d_P^2 + d_P'^2 + d_P''^2 \quad \sim \quad -1 + f^{2/3} + (1-f)^{2/3} \tag{9}$$

For equal sized breakage, the maximum additional interfacial energy ΔE_{max} is necessary and the probability density function is at its minimum. On the other hand, the highest probability density is obtained for the most unequal daughter drop sizes, resulting in a U-shaped distribution. The dimensionless daughter drop size distribution, which is normalized by its integral over f, is given as follows:

$$\beta(f,1) = \frac{\Delta E_{max} - (\Delta E(f) - \Delta E_{min})}{\int_0^1 \left[\Delta E_{max} - (\Delta E(f) - \Delta E_{min})\right] df} \tag{10}$$

The minimum additional interfacial energy ΔE_{min} is needed if one daughter drop is of the smallest possible size d_{min}. Tsouris and Tavlarides [21] were not clear about how this minimal drop size could be determined. In fact, from the short explanations in their article, one could conclude that it was only introduced to avoid problems with numerical calculations and set to zero. In this way, Tsouris and Tavlarides [21] were interpreted by various authors, for example by Liao and Lucas [8].

However, the assumption of a minimal drop size is retained in the present article, supported by empirical data. This value can either be taken from the minimal drop diameter experimentally detected in the liquid-liquid dispersion, i.e. $d_{min} = 10$ µm, or if no data is available, it is set equal to the minimum eddy size in the Kolmogorov length scale. In this interpretation, the probability density of Tsouris and Tavlarides does not become zero for equal sized breakage, in contrast to presentations by Liao and Lucas [8]. Additionally, it depends on the mother drop diameter becoming flatter for small mother drops.

2.2.3 The model of Lehr, Millies and Mewes

Lehr et al. [22] subscribe to the assumption of many authors, e. g. Luo and Svendsen [23], that the size of the bombarding eddy must be smaller than the mother drop diameter in order to be distorted. In addition, they postulate, that the eddy must not be smaller than the smallest daughter drop to carry this daughter drop away. The eventual sizes of the daughter drops depend of the kinetic energy of the eddy being equal to the interfacial energy of the smaller daughter drop. However, because of the capillary pressure increasing for decreasing drop diameters, Lehr et al. [22] reason that bigger fragments are more probable than small ones.

On the other hand, the authors assume that the velocity of the eddies, and thus their kinetic energy, is Gaussian-distributed around the mean eddy velocity of $\sqrt{2}(\varepsilon\lambda)^{1/3}$ and that the eddy number density is proportional to λ^{-4}, following Luo and Svendsen [23] and Hinze [24]. Lehr et al. [22] conclude that big mother drops break most likely unequally while small drops result in equal breakage most probably. This is because smaller eddies are large in number but often lack in enough kinetic energy to create very small drops with high capillary pressure. Therefore, the daughter drop size distribution is bell-shaped for small mother drops, becomes M-shaped for bigger and finally U-shaped for very big mother drops.

The dimensionless daughter drop size probability function can be expressed as normalized lognormal distribution of the dimensionless daughter drop diameter $d_P^* = d\gamma^{-3/5}\rho_c^{3/5}\varepsilon^{2/5}$ as follows:

$$\beta(f,1) = \frac{1}{2\sqrt{\pi}f} \frac{\exp\left(-\frac{9}{4}\left[\ln(2^{2/5}d'^{*})\right]^2\right)}{\operatorname{erfc}\left[-\frac{3}{2}\ln(2^{1/15}d^{*})\right]} \quad \text{for} \quad f \le 0.5$$
$$\beta(1-f,1) = \beta(f,1) \quad \text{for} \quad f > 0.5 \tag{11}$$

The daughter drop size distribution also has to be mirrored at $f = 0.5$ and is similar to the equation given by Liao and Lucas [8]. However, two mathematical modifications were made: In order to meet the normalization condition, the distribution was divided by 2, verified by numerical integration. Furthermore, numerical problems occurred because of the error function in the original equation, now being replaced by the error function complement after a few mathematical transformations.

3 MATERIAL AND METHODS

This research utilized two main set-ups: a single drop breakage cell [25] and an agitated vessel at lab scale [26]. Both have been used in previous studies.

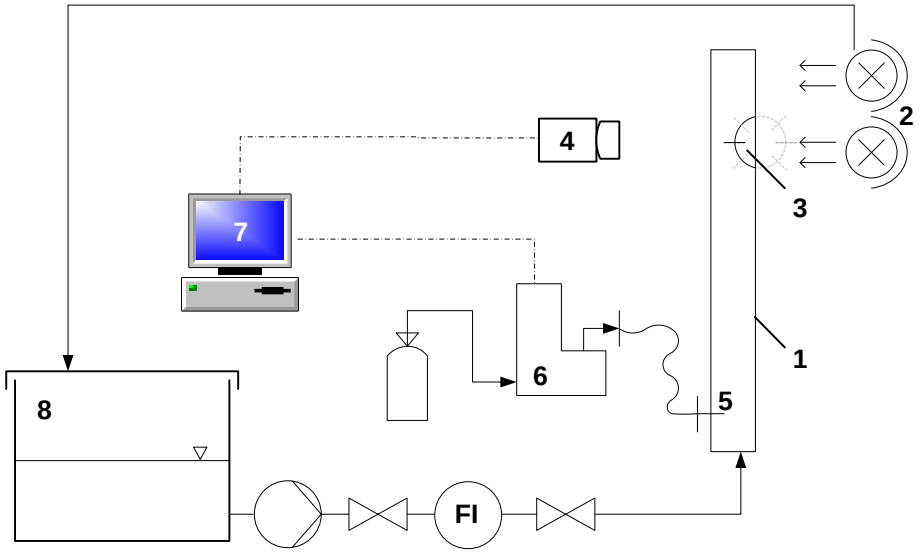

Figure 1 – Experimental set-up for single drop experiments: (1) breakage cell, (2) illumination, (3) section of a Rushton turbine, (4) highspeed camera; (5) nozzle for drop formation, (6) precision dosing pump, (7) computer control, (8) water storage tank

3.1 Single drop experiments

The drop breakage cell allows single particle breakage experiments separately from coalescence phenomena. A single blade representative for a section of a Rushton turbine is fixed in a rectangular channel (see Figure 1). This set-up emulates the flow field in the impeller region. The relative velocity between blade and liquid flow was approximately 1.0 to 3.0 m/s. The mother drop sizes have been set between 500 and 3500 µm. High accurate dosing pump produces mother drops with standard deviation of the diameter less than 0.003 mm [25].

Pictures of the single drop breakage event and the resulting daughter drops are taken with a high-speed camera using a frame rate of 822 frames per second (fps). Automated image recognition delivers results for the number and size of daughter drops (see Figure 2). The different steps of image processing and analysis are described in detail by Maaß et al. [27].

Figure 2 shows a breakage sequence of a breaking 2 mm toluene mother drop for 1.5 m/s. The flow direction is displayed in frame 14 of the set. Although the drop is extremely elongated and stretched, the first breakage occurring is a binary (see frame 14 in Figure 2). The second number behind the image number on each frame displays the number of particles counted in those images. The number of particles is increasing over time. This breakage cascade leads to the maximum number of drops at one image in frame 23 with 27 particles. However, the breakage events in PBE simulations are modeled by every single breakage event. Therefore, only the initial breakage events are analyzed and presented in this study. While the counting of the number of fragments is trivial, the daughter drop size distribution needs more attention to be determined. Only binary breakages were analyzed for the DDSD.

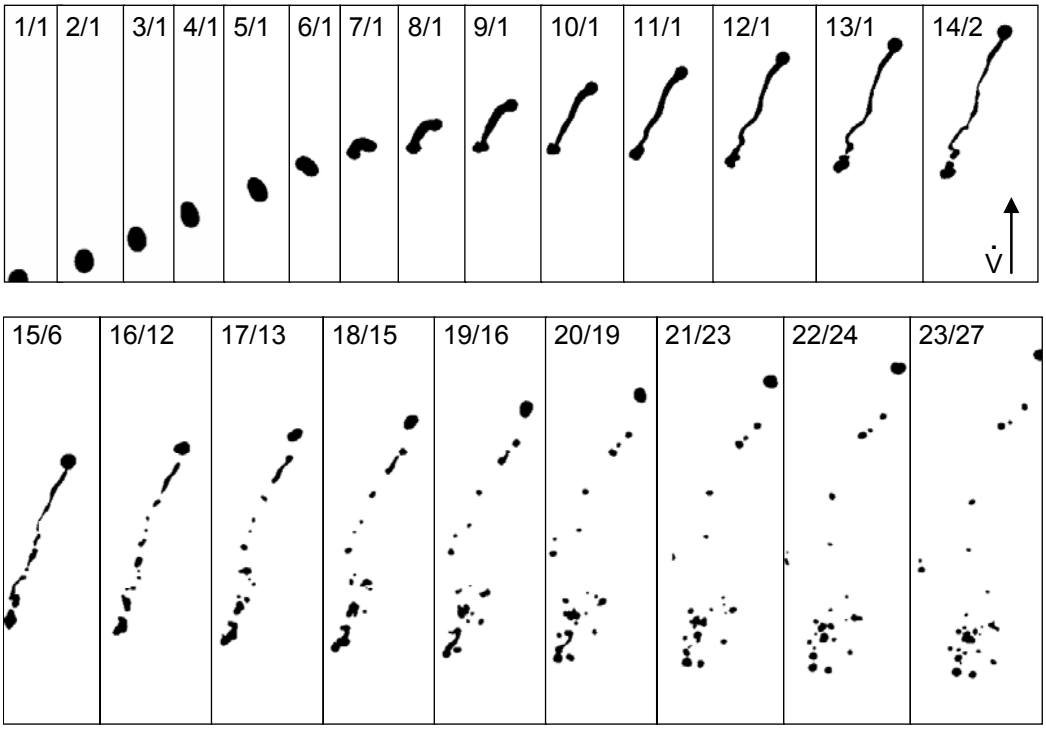

Figure 2 – Example initial binary breakage with following break-up cascade of 2 mm toluene drop, always with the image number/ number of particles on the image

From the areas by which the drops are represented on the pictures the volumes of the mother drops and of the smallest daughter drops were calculated by image analysis. The second daughter drop volume, which is presumably more distorted, as can be seen in Figure 2, was calculated by means of mass balance. Finally, splitting up the dimensionless daughter to mother drop volume ratio $f = V'_P/V_P$ into 50 intervals, the numbers of events for each interval

were counted. The empirically determined distribution was turned dimensionless, being divided by its numerical integral over f.

Toluene (99.98 % purity) and petroleum (99.9 % purity) were used as dispersed phase for the single drop investigation. Both were blended with a non-water soluble black dye. The physical properties for the used media are listed in Table 2.

3.2 Stirred vessel

Figure 3 and Table 3 show the main features of the selected stirred vessel, used for the drop swarm experiments. All geometrical parameters were kept constant for all experiments, including the flat blade impeller.

Toluene/water was used as the model system. To avoid coalescence in the drop swarm experiments high concentrations of polyvinyl alcohol (PVA) have been used. The emulsion was stabilized with 3 mg of PVA per used 1 g of toluene. The interfacial tension at this concentration is 4.4 mN/m. It was determined with the pendant drop and the ring method. The physical properties are given in Table 2.

Table 2 – Properties of used chemicals

	γ [mN/m]	γ [mN/m] with dye	γ [mN/m] with PVA	ρ [kg/m³] at 20°C	η_d [mPa·s]
toluene	36	32	4.4	870	0.55
petroleum	42	38.5	-	790	0.65

The transient drop size distributions (DSD) are determined using an in-situ photo optical method [28] with automatic drop detection [29]. This endoscope technique is used in various studies as a trustful method for validation of other measurement techniques [28, 30]. To evaluate the coalescence behavior under the selected conditions the liquid-liquid system was first dispersed at 410 rpm for several hours. After 11 h of mixing the stirrer speed was decreased to 250 rpm and the drop size was still measured. While no drop size increase after the stirrer speed decrease was determinable, the coalescence efficiency is assumed to be zero. This is in good agreement with previous studies where even lower surfactant concentrations were used [31].

Table 3 – Dimensions of the used stirred tank

T	H/T	l_B/T	D/T	h/D	h_{St}/D	w_B/T	Ne [-]
155 mm	1.4	1.0	0.6	1.8	0.06	0.08	0.21

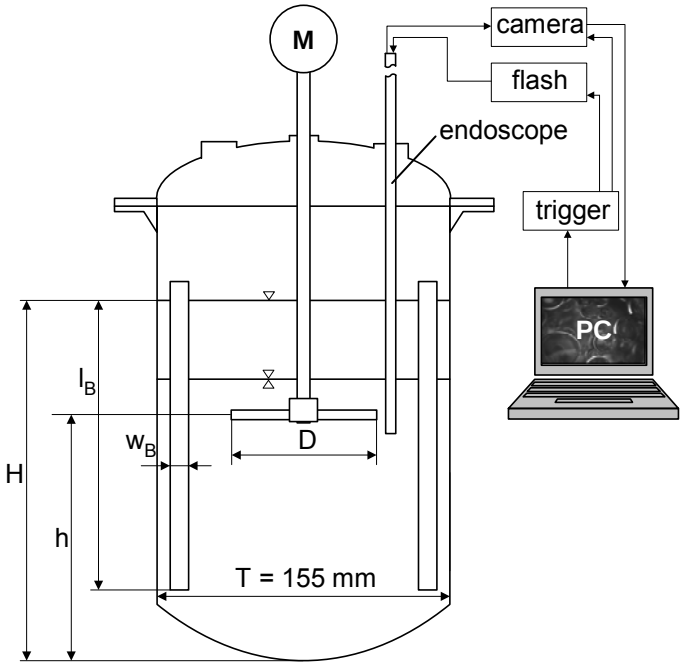

Figure 3 – Experimental set-up and dimensions of the used stirred tank

3.3 Numerical scheme

The population balance equation is applied with the intention to calculate the transient drop size distribution in the stirred liquid/liquid system. A major result from previous studies are the necessity for the use of a two-zone model to meet the needs occurring with the extreme inhomogeneities of the local energy dissipation in agitated reactors [26]. Therefore, only the two-zone modeling approach was considered for simulations of drop sizes in the investigated vessels. One zone describes the stirrer region with high energy dissipation rates ε. This zone is comparable with the volume around the stirrer blade of the single drop breakage cell. The second zone describes the bulk region, which is the large region outside the stirrer region.

Based on the experimental results of the transient drop sizes no coalescence kernel was taken into account for the simulations. Different daughter drop size distributions have been tested always combined with the breakage rate from Coulaloglou and Tavlarides [9]. The number of daughter drops will be fixed to a priori. This value will be based on the following single drop results.

The two free parameters in the used breakage rate have been always estimated for every different daughter drop size distribution using the numerical solver PARSIVAL® [32]. This estimation uses a damped Gauss-Newton method to minimize the differences between calculated and experimental values of the Sauter mean diameter ($d_{32} = \Sigma\, d_{P,i}^3/\Sigma d_{P,i}^2$) for every measured time step.

4 Results and Discussion

The breakage of a parent drop d_P into two daughter drops d_P' and d_P'' is assumed in most investigations [33]. The choice of the number of daughter particles directly influences the other breakage model parts in the PBM framework [18]. It is obvious, that the change of ν or the

daughter drops size distribution $\beta(d_p,d_p')$ will directly affect the breakage rate $g(d_P)$ and therewith always the used numerical parameters. The single drop breakage experiments are used to determine precise knowledge about these terms. The results are presented in the next two sections. The experiences from these single drop breakage results are used in the last section of this chapter to simulate the evolution of an agitated liquid-liquid system.

4.1 Single drop experiments – number of daughter drops

The experimentally determined number of daughter particles during the first breakage event of single toluene drops is presented as a function of the mother drop diameter for a constant flow velocity in Figure 4. As a general trend, the initial number of daughter drops is decreasing with increasing mother drop diameter. The table in Figure 4 also displays the average number of particles out of all breakage events for a constant flow velocity and a mother drop diameter of a given size. This average number is the arithmetic average value which can be directly calculated from the presented distribution of events over ν.

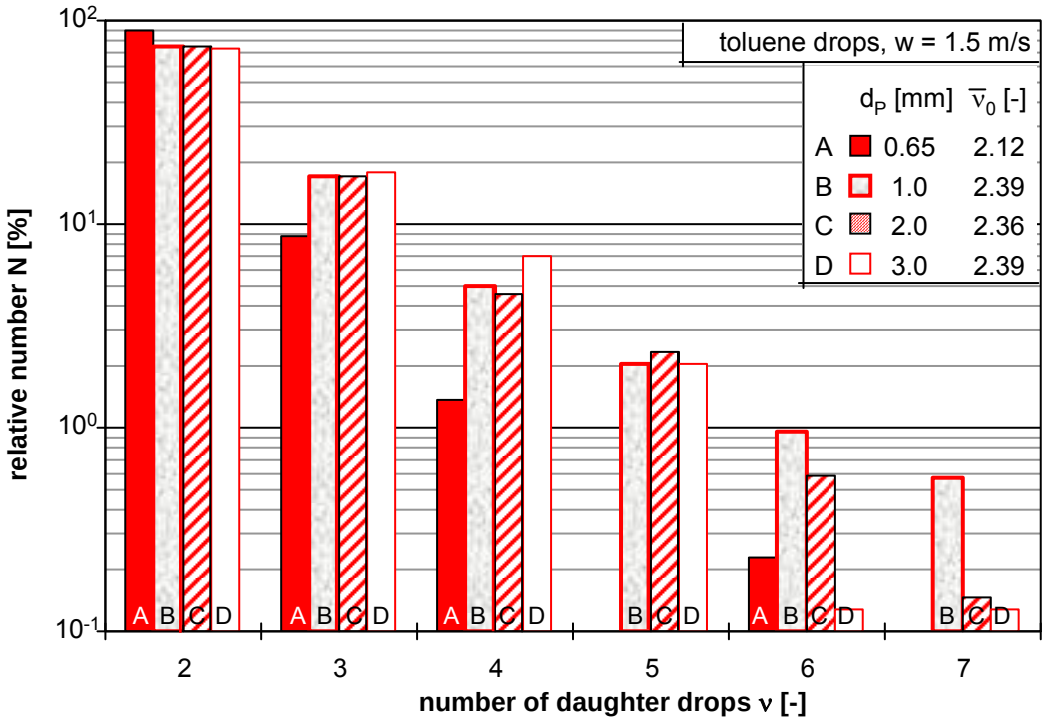

Figure 4 – Relative number distribution of the number of daughter drops after the first breakage event resulting from various toluene drops

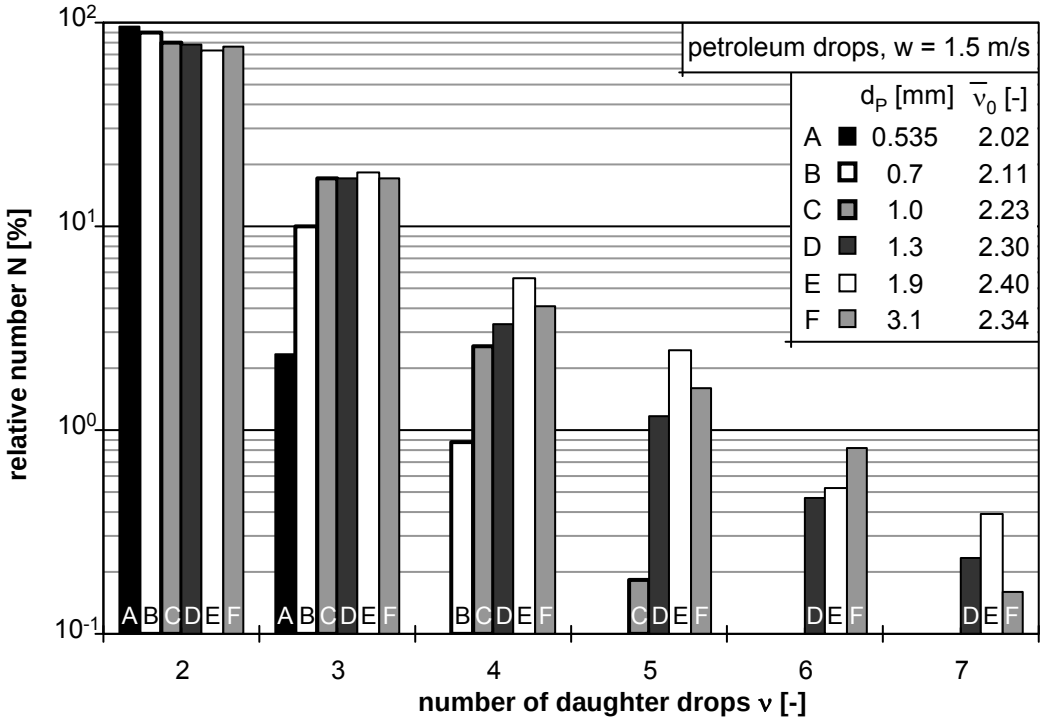

Figure 5 – Relative number distribution of the number of daughter drops after the first breakage event resulting from various petroleum drops

The same tendencies as for the toluene drops can be found for the petroleum drops which are presented in Figure 5. For the smallest investigated drop diameter (d_P = 0.535 mm) the probability for an initial binary breakage is over 95%. This probability is decreasing to almost 70% for the 3.1 mm petroleum drops. Note that for the toluene drops of a comparable size to the petroleum drops, the number of daughter fragments is always slightly higher. The physical specifications show lower interfacial tension and lower viscosities for the toluene/water system compared to petroleum/water. This leads to lower surface energy and deforming resistance. So it is easier to break toluene than petroleum drops which is displayed in the higher number of daughter drops for a constant frame rate.

Table 4 – Influence of frame rate on number of daughter drops for 1 mm toluene drops at 1.5 m/s

frame rate [fps]	probability of binary breakage	average number at initial breakage $n_{0,av}$ [-]	max. number at initial breakage $n_{0,max}$ [-]
125	0.45	3.82	27
500	0.62	2.83	8
822	0.74	2.39	7
1450	0.88	2.15	4

A sensitivity analysis of the frame rate showed the influence of the used measurement technique on the achieved results. The results are given in Table 4. With increasing the frame rate of the used camera the number of binary breakages after the first breakage event increases and vice versa for the decrease of the frame rate. That means, that most probably all ternary or higher breakage events are a cascade of binary breakages. To observe this, a much higher time resolution is necessary than the used one.

Concluding the results of the single drop experiments on the number of daughter drops, the use of binary breakage in population balance modeling appears obvious. Therefore, only binary breakage is assumed in the PBE simulations carried out in this study. To gain further insides on the breakage phenomena and their necessary description in the PBE, the daughter drop size distribution will be analyzed in the next section.

4.2 Single drop experiments – daughter drop size distributions

In Figure 6 and Figure 7 the experimentally determined dimensionless daughter drop size distributions are displayed for two different mother drop diameter (d_P = 1,0 and 0.644 mm). They are along with the theoretical distributions from chapter 2 which were calculated for the given experimental conditions. The experimental values are broadly distributed opposed to the most quoted assumption of a Gaussian distribution. Concretely the breakage into a very small and a very large daughter drop seems most probable.

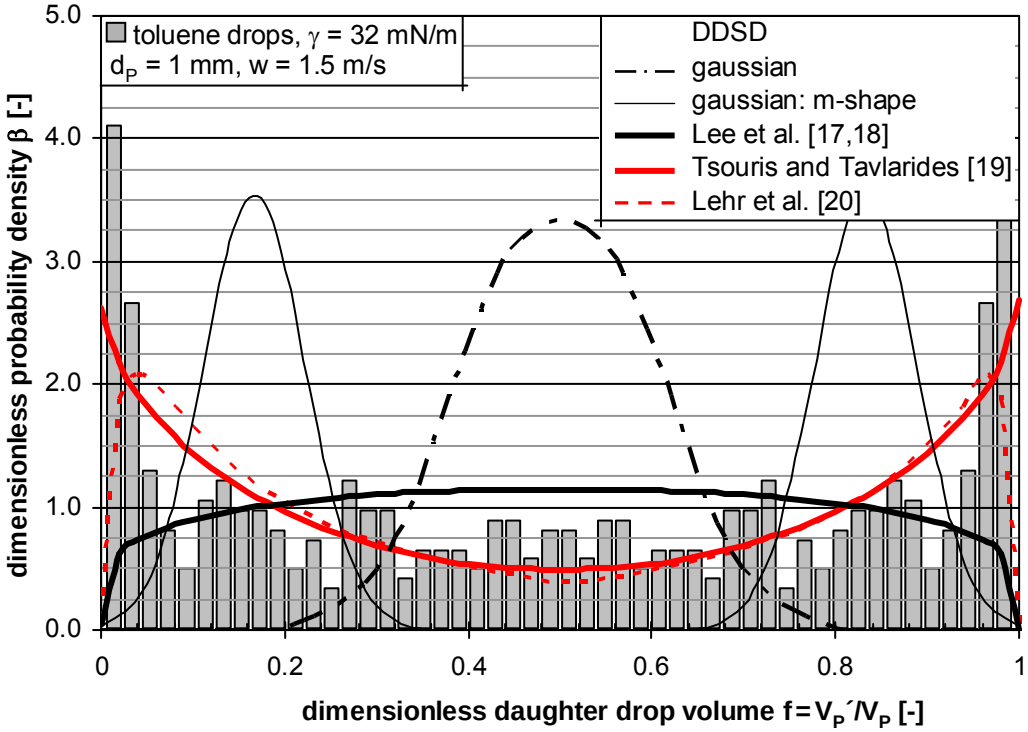

Figure 6 – Experimental and theoretical DDSD for 1 mm toluene drops

In Figure 7, no breakages are displayed for the smallest and the largest size interval of the volume ratio f. Thus, for the mother drop diameter of 644 µm, the limitation of measurability by means of the described equipment already becomes obvious. Due to the resolution of the camera, breakage could not be detected, if one daughter drop had a diameter which was below 100 µm (f = 0.004 for d_P = 644 µm) which equals to the length of one pixel. Furthermore, if a very small drop was situated at the border of two or more pixels, it maybe also was not detected. Therefore, only daughter drops which were bigger than two pixels, i.e. 200 µm (f = 0.03), were captured by the camera for sure. However, the comparison of the experimental results from Figure 6 and Figure 7 gives some first insights. The distribution of daughter drops in the investigated size range should rather be displayed by a bimodal distribution. Therefore, the two phenomenological models (Tsouris and Tavlarides [21] and Lehr et al. [22]) show the best agreements with the experimental values. The β-distribution by Lee et al. [19] shows also quite satisfying results. Only the values for the smallest and the largest intervals are contrary to the experiments.

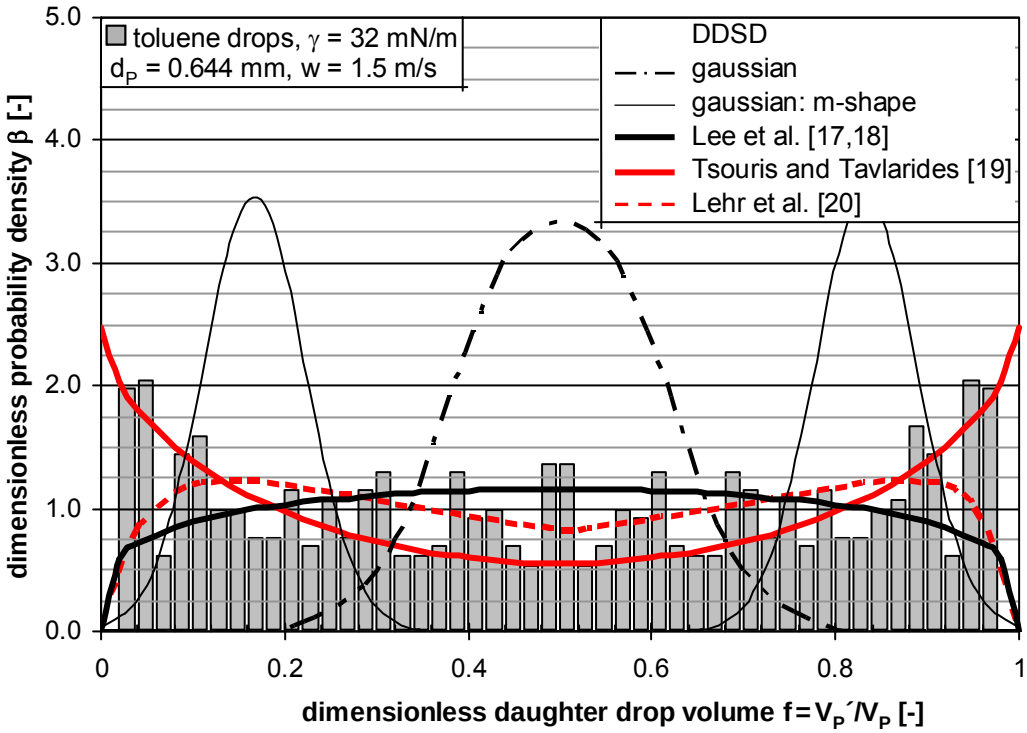

Figure 7 – Experimental and theoretical DDSD for 644 µm toluene drops

In Figure 8, the differing influence of the mother drop diameter for each theoretical daughter drop size distribution is shown. While the distribution of Lehr et al. [22] varies strongly, no changes can be observed for the statistical distributions and only a small change for the model of Tsouris and Tavlarides [21]. In comparison to Figure 7, the great impact of the interface tension for the model of Lehr at al. [22] becomes visible by comparing the shape of this distribution. For a constant mother drop diameter of 0.644 mm the decrease in the interfacial

tension from 32 to 4.4 N/m leads to an extreme bimodal DDSD (compare Figure 7 and Figure 8 upper left plot). The probability for equal sized breakage is zero and the breakage into a very large and a very small drop becomes most probable. This shape varies strongly over the mother drop diameter until it turns into a bell-shaped DDSD for small drops. For the 0.12 mm mother drop the distribution by Lehr et al. [22] is comparable to the presented β-distribution and finally turns into a form which is almost comparable to the Gaussian one.

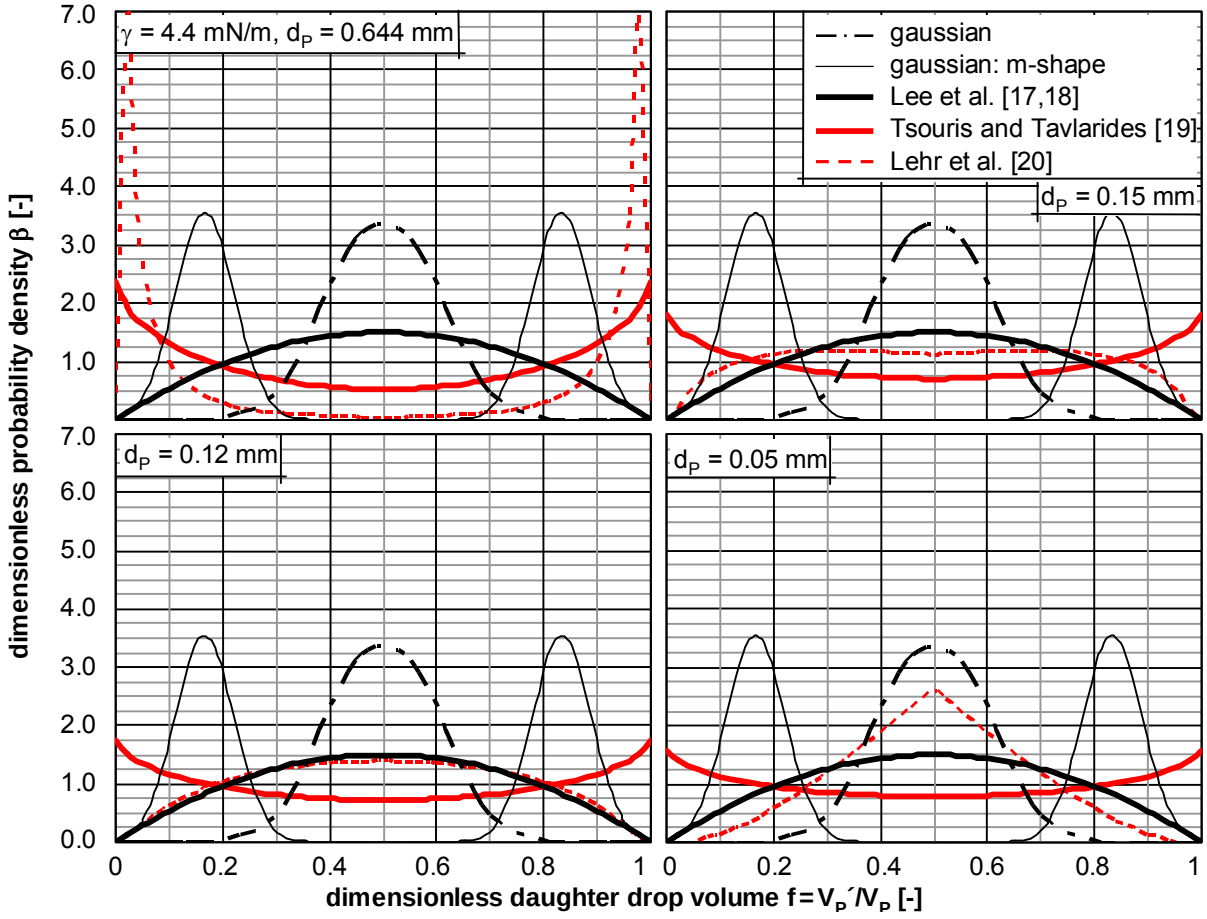

Figure 8 – Influence of mother drop diameter on several DDSD

For the interpretation of the model of Tsouris and Tavlarides [21] employed in the present paper, the minimal drop diameter was set equal to the minimal eddy size of the Kolmogorov length scale. This assumption is open to discussion. Probably, the value is too small, since the drop deforming eddies are supposed to be in the inertial sub-range which contains sufficient kinetic energy and is about one order of magnitude above the Kolmogorov length scale [23]. The way employed here to calculate the smallest possible drop is rather pragmatic, referring to the assumption that deformations of mother drops occur only, if there are eddies of appropriate size causing them [22]. In highly turbulent systems the deformations of drops are assumed to be created by the velocity fluctuations in the fluid. According to Lehr et al. [22], the deformations of the mother drop determine the size of the daughter drops. Assuming, that

drop breakage is caused by a cascade of bombarding eddies; the resulting daughter drops cannot be smaller than the smallest distorting eddy.

The results of the daughter drop size distribution analysis can be concluded as follows: The experimental DDSD show a clear tendency to unequal sized breakage. The development of the U-shape for bigger mother drops to a flatter U-curve, which could become M-shaped and even bell-shaped, is suspected but yet has to be proven experimentally. However, according to the assumptions of the phenomenological daughter drop size distributions which were sketched in chapter 2, the shape of the experimental distributions can be interpreted in such a way that the interfacial energy [21] and/or the distributions of eddy sizes and kinetic energies [23] account for the daughter drop sizes. Future single drop experiments, employing a higher-resolution high-speed camera, or other experimental conditions, are to discover whether the U-shape develops into the M-shape and a bell-shape respectively, as proposed by Lehr et al. [22]. In the mean time, drop size distributions of coalescence hindered stirred-vessel experiments could give an insight into the daughter drop size distributions of smaller drops, as will be suggested in the next section.

4.3 PBE simulations

Based on the single drop experiments, different daughter drop size distributions are used to simulate the transient behavior of the agitated toluene/water system. As parameter identification is always very challenging, values from literature have been used first. Maaß and Kraume [34] have been determined values for the two numerical constants $c_{1,b}$ and $c_{2,b}$ (see equation (3)) very precisely based on single drop experiments (see Table 5). Simulation results for the transient Sauter mean diameters are presented in Figure 9. The simulations are compared with experimental values.

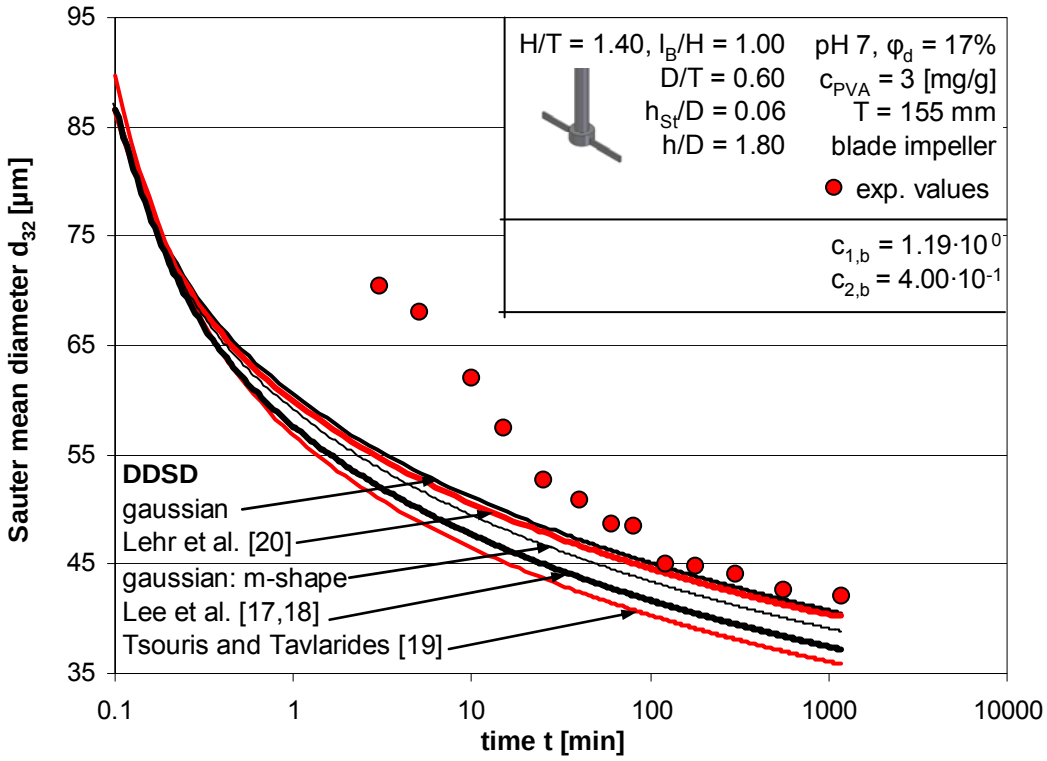

Figure 9 – Comparison of experimental determined transient Sauter mean diameter and PBE simulations using several DDSD

All curves show the same major trend - with increasing agitation time the drop sizes are decreasing. Interestingly the differences between the different simulations using different daughter drop size distributions are relatively low opposed to their shape (for comparison see Figure 8). All simulations over predict the drop size evolution, especially in the first hour of the process. Although the differences between the simulation results are low, the model using a Gaussian daughter drop size distribution shows the best results compared to the experimental values. This model approach is predicting the Sauter mean diameter for the steady state condition after 1170 min of mixing. Prediction results of comparable empirical correlations reported in literature have not been that precise without parameter adjustment [6]. However, for a precise simulation of the transient process behavior a parameter optimization is still necessary.

As it is not only important to get knowledge about a mean diameter of the dispersed phase the cumulative number distributions over time are analyzed. For a clear evaluation of the prediction capacity of each DDSD used in the presented PBE-model, both numerical constants ($c_{1,b}$ and $c_{2,b}$ – see equation (3)) have been estimated. Therefore, the coefficient of determination R^2 describing the deviations between experiments and simulations has been maximized for each model. The constant results are given in Table 5. All model combinations have been very successfully fitted against the experimental results as the R^2-values are always higher than 0.982 (see Table 5). The optimized parameters have been used for all following simulations.

Table 5 – Optimized numerical constants for different daughter drop size distributions

DDSD	$c_{1,b}$ [-]	$c_{2,b}$ [-]	R^2 [-]
Gaussian	$1.19 \cdot 10^{-2}$	$2.75 \cdot 10^{-1}$	0.988
Gaussian – m-shape	$1.70 \cdot 10^{-2}$	$3.00 \cdot 10^{-1}$	0.983
Lee et al. [19]	$1.80 \cdot 10^{-2}$	$3.00 \cdot 10^{-1}$	0.982
Tsouris and Tavlarides [21]	$3.70 \cdot 10^{-2}$	$3.60 \cdot 10^{-1}$	0.986
Lehr et al. [22]	$1.55 \cdot 10^{-1}$	$2.85 \cdot 10^{-1}$	0.991
literature values from single drop experiments:			
Maaß and Kraume [34]	$9.1 \cdot 10^{-1}$	$3.90 \cdot 10^{-1}$	-

The experimental results for four different points in time are compared in Figure 10 with simulations using a Gaussian daughter drop size distribution. Both reflect the decrease of the drop size over time during agitation. Besides the good prediction of the general trend of the drop size evolution, the simulation fails to reflect the experimental determined shape of the distribution. The measured distributions are much wider than the calculated ones.

Reviewing possible influence parameters on the shape of the distribution, the initial distribution is proposed [35]. Three different initial distributions have been used to determine the dependency of the transient distribution on this numerical parameter. Therefore, two experimentally determined distributions and one theoretical lognormal distribution are used for simulations using the presented PBE model with a Gaussian daughter drop size distribution. The transient simulation results of the Sauter mean diameter and the standard deviation achieved with the different initial distributions are given in Table 6. Although the initial conditions vary significantly, the simulated drop size distributions for a process time larger than three minutes do not. That shows the insensitivity of the simulations on the initial condition. While this is promising in terms of reliability of the population balance method, it does not solve the problem of determining the influence parameters on the shape of the drop size distributions.

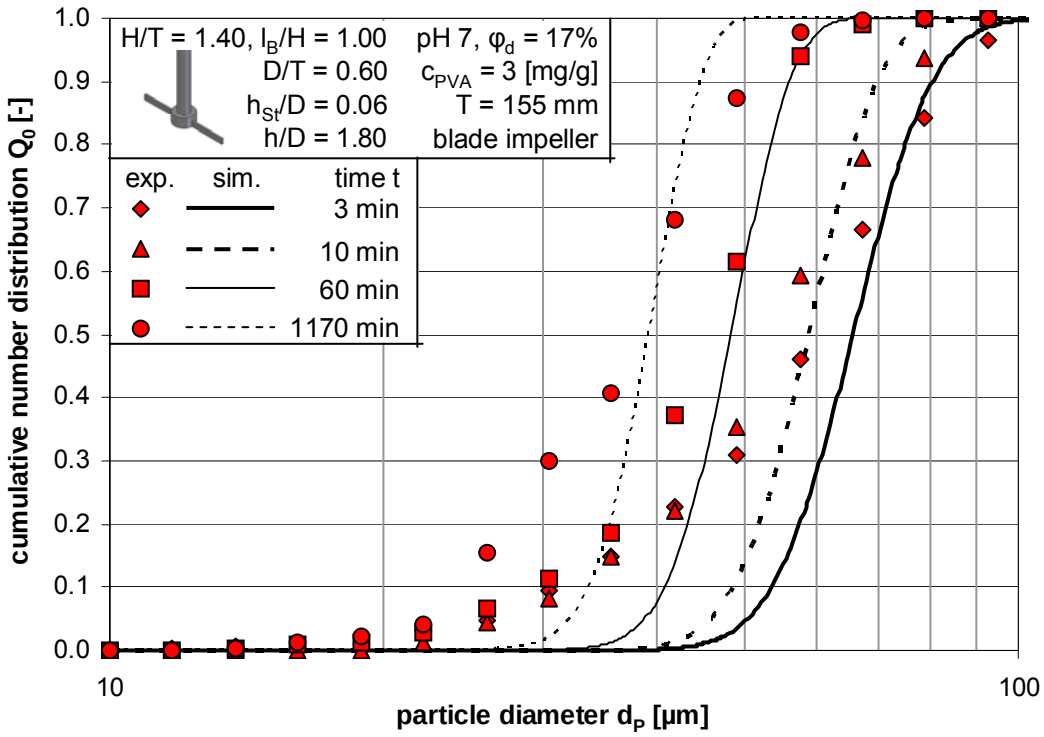

Figure 10 – Comparison of experimental determined transient drop size distribution and PBE simulations using a Gaussian daughter drop size distribution

Table 6 – Comparison of the simulated drop sizes and standard deviations using different initial distributions

type of distribution	initial stage		t = 5 min		t = 1170 min	
	d_{32} [µm]	σ [µm]	d_{32} [µm]	σ [µm]	d_{32} [µm]	σ [µm]
experimental	170	115.3	70	18.3	40	6.2
experimental	340	223.5	70	18.4	40	6.2
lognormal	870	504.1	73	19.1	40	6.2

Discussion in literature proposes other key parameters in modeling, influencing the shape of the distribution [20]. Resulting transient drop size distributions by the use of different daughter drop size distributions are compared with experimental values in Figure 11. The five simulated distributions, using five different daughter drop size distributions, show different results for a single point in time.

The results can be summarized as follows:

- the Gaussian distribution leads always to too narrow distributions
- opposed, the DDSD after Tsouris and Tavlarides [21] leads always to too wide distributions

- the simulated DSD using the DDSD after Lehr et al. [22] becomes more narrow over time
- the β-distribution after Lee et al. [19] and the m-shaped Gaussian distribution give the best results

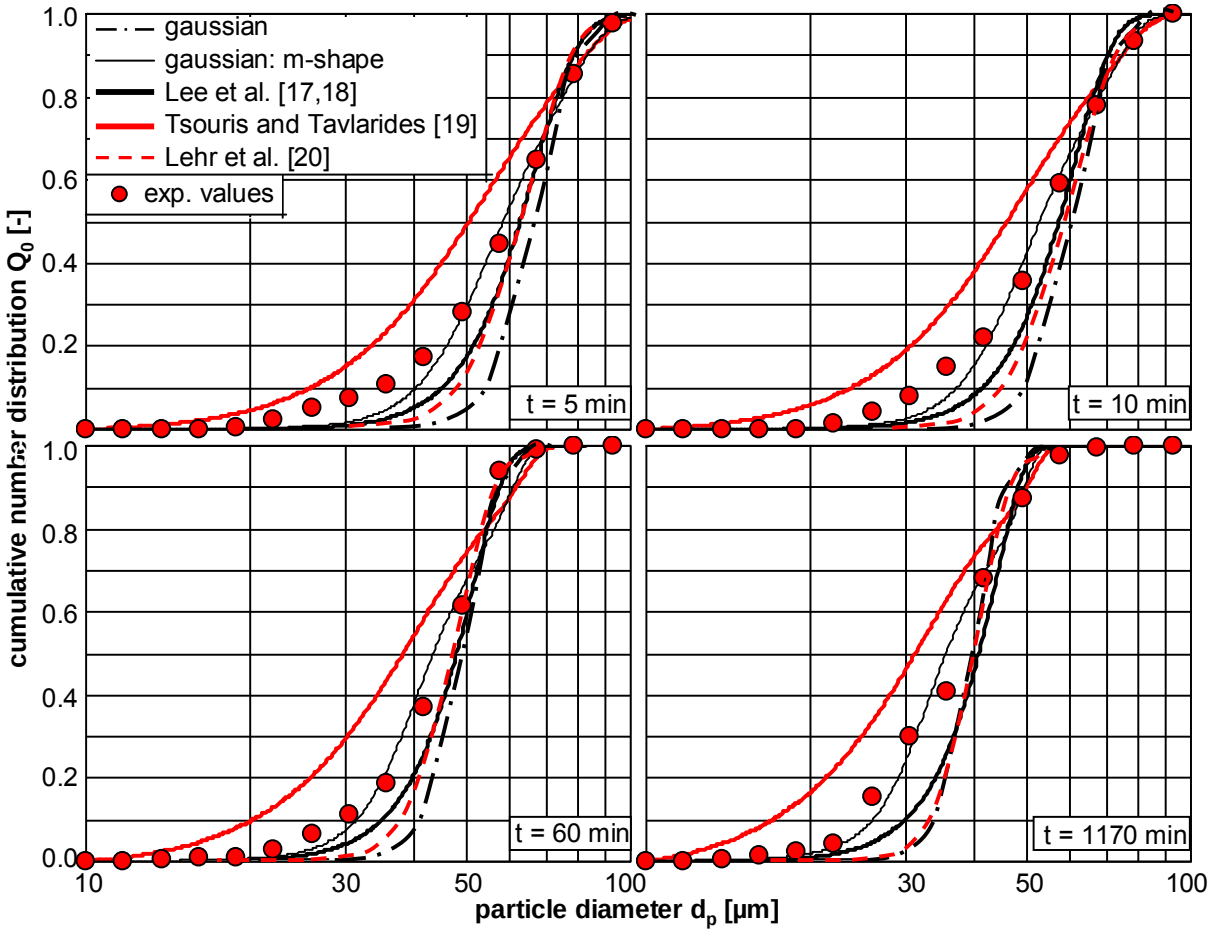

Figure 11 – Comparison of an experimental determined cumulative number density distribution and PBE simulations using several DDSD

The comparison of the shape of the different DDSD (see Figure 8) with the resulting DSD over time reveals the strong connection of these influence parameters. The U-shaped distribution from Tsouris and Tavlarides [21] has to produce the widest drop size distributions. The high probability for very small and very large daughter particles is favoring broad distributions.

The DDSD by Lehr et al. shows the strongest variation in its shape over the diameter. Therewith it shows the strongest variation of the resulting DSD over time due to the size decrease.

5 CONCLUDING REMARKS

Understanding and predicting of particle strain is relevant for various technical applications. In this study a simplification is carried out. To analyze particle strain single drop experiments in a breakage cell and evolving drop size distributions in an agitated, breakage dominated system are studied. The mechanisms for particle strain and drop breakage are assumed to be comparable for the investigated turbulent flow regime. The agitation process is simulated using a population balance model. This model provides transient prediction capacities at different scales and therefore, can be used for scale-up or scale-down projects.

The single drop experiments provide necessary information, whose are needed within the population balance equations for a proper system characterization. The number of daughter fragments for single drops at constant flow velocity for various mother drop diameter and two different solvents have been studied. The results clearly support the assumption of binary breakage, often used in literature. Even the appearance of multiple daughter drops or the creation of satellite drops can be separated into a cascade of binary breakage events. Ultra high time resolution is necessary for this kind of analysis.

The daughter drop size distribution for such binary breakages is studied for the toluene/water system and two different mother drops. The comparison with various literature models for the DDSD shows that bimodal or at least very broad bell-shaped distributions of the daughter drops should be used for the modeling. The most common assumption of a Gaussian distribution could not be supported.

These detail information of breaking drops were used to provide necessary information within the population balance. The evolution of a breakage dominated toluene/water system was than simulated using different daughter drop size distributions. The computational results were than compared with experimental values. All simulations were able to predict the transient Sauter mean diameter excellent after parameter fitting. The prediction of the transient drop size distribution was more complex to evaluate. The use of different DDSD had an intense influence not on the mean diameter but on the shape of the distribution. The Gaussian distribution lead always to too narrow distributions, opposed the DDSD after Tsouris and Tavlarides [21]. This DDSD lead always to too wide distributions. The β-distribution after Lee et al. [19] and the m-shaped Gaussian distribution gave the best results with advantages in preciseness for the M-shaped Gaussian distribution. The differences in the simulated drop size distributions in the agitated vessel are in meaningful agreement to the original shape of the daughter drop size distribution.

Although these results were obtained in a particular vessel for a specific phase system it can be applied to simulate transient multiphase systems at different scales. We would expect that the general trends observed in this study are comparable to various applications in multiphase bioreactors.

LATIN SYMBOLS

a; b - parameter for the β-distribution [-]

c - tolerance limit for the Gaussian distribution [-]

$c_{1,b}$; $c_{2,b}$ - numerical constants in the breakage rate [-]

d_P - drop diameter [m]

d_P'; d_P'' - drop diameter of the first and the second daughter drop [m]

D - stirrer diameter [m]

$D_{b;c}$ - sink term of breakage or coalescence [1/s]

d_{32} - Sauter mean diameter [m]

E - energy [J]

f - daughter to mother drop volume ratio [-]

g - breakage rate [1/s]

h - bottom clearance, stirrer height [m]

l_B - baffle length [m]

H - liquid level [m]

n - stirrer speed [rpm]

N - relative number of events [%]

Ne - Power or Newton number [-]

Q_0 - cumulative number distribution [-]

$S_{b;c}$ - source term of breakage or coalescence [1/s]

t - time [s]

T - tank diameter [m]

V_P - drop volume [m^3]

V_P'; V_P'' - drop volume of the first and the second daughter drop [m^3]

w - velocity [m/s]

GREEK SYMBOLS

β - beta distribution (a general statistical distribution)

β - daughter drop size distribution

γ - interfacial tension [mN/m]

ε - P/V - energy dissipation rate [W/m^3]

η - dynamic viscosity [kg/(m·s)]

λ - Kolmogoroff length [m]

μ - expectation value of a Gaussian distribution

ν - kinematic viscosity [m^2/s]

ν - number of daughter drops [-]

ρ - density [kg/m^3]

φ - dispersed phase fraction [-]

σ - standard deviation

SUBSCRIPTS

b - breakage

c - continuous phase

c - coalescence

crit - critical value

d - dispersed phase

max - maximum value

min - minimum value

st - stirrer

* - dimensionless value

ABBREVIATIONS

DSD - drop size distribution

DDSD - daughter drop size distribution

fps - frames per second

PBE - population balance equation

PVA - polyvinyl alcohol

PVC - polyvinyl chloride

ACKNOWLEDGEMENTS

The authors gratefully acknowledge Ms. Tina Skale and Ms. Melanie Zillmer for the support, performing the single drop experiments and Ms. Miriam Bezeran Sauras for the support with the experiments in the stirred vessel. The financial support by the Max-Buchner-Forschungstiftung and the Deutsche Forschungsgemeinschaft (DFG) via the project „Modelling, Simulation, and Control of Drop Size Distributions in stirred Liquid/liquid systems" is gratefully acknowledged.

LITERATURE

[1] Wollny, S., *Experimentelle und numerische Untersuchungen zur Partikelbeanspruchung in gerührten (Bio-)Reaktoren*, phd-thesis, Technische Universität Berlin, 2010, pp. 177 (in German).
[2] Henzler, H.-J., Particle Stress in Bioreactors, *Influence of Stress on Cell Growth and Product Formation*, Springer Berlin / Heidelberg 2000, pp. 35-82.
[3] Ghadge, R. S., Patwardhan, A. W., Sawant, S. B., Joshi, J. B., Effect of flow pattern on cellulase deactivation in stirred tank bioreactors. *Chem. Eng. Sci.* 2005, *60*, 1067-1083.
[4] Eibl, R., Eibl, D., Pörtner, R., Catapano, G., Czermak, P., *Cell and Tissue Reaction Engineering*, Springer-Verlag, Berlin / Heidelberg 2009.
[5] Galindo, E., Pacek, A. W., Nienow, A. W., Study of drop and bubble sizes in a simulated mycelial fermentation broth of up to four phases. *Biotechnol. Bioeng.* 2000, *69*, 213-221.
[6] Cull, S. G., Lovick, J. W., Lye, G. J., Angeli, P., Scale-down studies on the hydrodynamics of two-liquid phase biocatalytic reactors. *Bioprocess. Biosyst. Eng.* 2002, *25*, 143-153.
[7] Azizi, F., Al Taweel, A. M., Algorithm for the accurate numerical solution of PBE for drop breakup and coalescence under high shear rates. *Chem. Eng. Sci.* 2010, *65*, 6112-6127.
[8] Liao, Y., Lucas, D., A literature review of theoretical models for drop and bubble breakup in turbulent dispersions. *Chem. Eng. Sci.* 2009, *64*, 3389-3406.
[9] Coulaloglou, C. A., Tavlarides, L. L., Description of Interaction Processes in Agitated Liquid-Liquid Dispersions. *Chem. Eng. Sci.* 1977, *32*, 1289-1297.
[10] Konno, M., Aoki, M., Saito, S., Scale Effect on Breakup Process in Liquid Liquid Agitated Tanks. *J. Chem. Eng. Jpn.* 1983, *16*, 312-319.
[11] Hesketh, R. P., Etchells, A. W., Russell, T. W. F., Experimental-Observations of Bubble Breakage in Turbulent-Flow. *Ind. Eng. Chem. Res.* 1991, *30*, 835-841.
[12] Bahmanyar, H., Slater, M. J., Studies of drop break-up in liquid-liquid systems in a rotating disc contactor. Part I: Conditions of no mass transfer. *Chem. Eng. Technol.* 1991, *14*, 79-89.
[13] Hancil, V., Rod, V., Break-up of a Drop in a Stirred Tank. *Chem. Eng. Process.* 1988, *23*, 189-193.
[14] Kuriyama, M., Ono, M., Tokanai, H., Konno, H., The Number of Daughter Drops Formed Per Breakup of a Highly Viscous Mother-Drop in Turbulent-Flow. *J. Chem. Eng. Jpn.* 1995, *28*, 477-479.
[15] Eastwood, C. D., Armi, L., Lasheras, J. C., The breakup of immiscible fluids in turbulent flows. *J. Fluid Mech.* 2004, *502*, 309-333.
[16] Galinat, S., Masbernat, O., Guiraud, P., Dalmazzone, C., Noik, C., Drop break-up in turbulent pipe flow downstream of a restriction. *Chem. Eng. Sci.* 2005, *60*, 6511-6528.
[17] Andersson, R., Andersson, B., On the breakup of fluid particles in turbulent flows. *AIChE J.* 2006, *52*, 2020-2030.
[18] Ramkrishna, D., *Population balances, theory and applications to particulate systems in engineering*, Academic Press, San Diego, CA 2000.
[19] Lee, C. H., Erickson, L. E., Glasgow, L. A., Bubble Breakup and Coalescence in Turbulent Gas-Liquid Dispersions. *Chem. Eng. Commun.* 1987, *59*, 65-84.
[20] Kostoglou, M., Dovas, S., Karabelas, A. J., On the steady-state size distribution of dispersions in breakage processes. *Chem. Eng. Sci.* 1997, *52*, 1285-1299.
[21] Tsouris, C., Tavlarides, L. L., Breakage and coalescence models for drops in turbulent dispersions. *AIChE J.* 1994, *40*, 395-406.
[22] Lehr, F., Millies, M., Mewes, D., Bubble-Size distributions and flow fields in bubble columns. *AIChE J.* 2002, *48*, 2426-2443.
[23] Luo, H., Svendsen, H. F., Theoretical model for drop and bubble breakup in turbulent dispersions. *AIChE J.* 1996, *42*, 1225-1233.
[24] Hinze, J. O., Fundamentals of the Hydrodynamic Mechanism of Splitting in Dispersion Processes. *AIChE J.* 1955, *1*, 289-295.
[25] Maaß, S., Wollny, S., Sperling, R., Kraume, M., Numerical and experimental analysis of particle strain and breakage in turbulent dispersions. *Chem. Eng. Res. Des.* 2009, *87*, 565–572.

[26] Maaß, S., Metz, F., Rehm, T., Kraume, M., Prediction of drop sizes for liquid-liquid systems in stirred slim reactors - Part I: Single stage impellers. *Chem. Eng. J.* 2010, *162*, 792-801.
[27] Maaß, S., Gäbler, A., Zaccone, A., Paschedag, A. R., Kraume, M., Experimental investigations and modelling of breakage phenomena in stirred liquid/liquid systems. *Chem. Eng. Res. Des.* 2007, *85*, 703-709.
[28] Maaß, S., Wollny, S., Voigt, A., Kraume, M., Experimental comparison of measurement techniques for drop size distributions in liquid/liquid dispersions. *Exp. Fluids* 2011, *50*, 259-269.
[29] Maaß, S., Rojahn, J., Hänsch, R., Kraume, M., Automated drop detection using image analysis for online particle size monitoring in multiphase systems. *Comput. Chem. Eng.* 2011, pp. 10.
[30] Lovick, J., Mouza, A. A., Paras, S. V., Lye, G. J., Angeli, P., Drop size distribution in highly concentrated liquid-liquid dispersions using a light back scattering method. *J. Chem. Technol. Biotechnol.* 2005, *80*, 545-552.
[31] Maaß, S., Rehm, T., Kraume, M., Prediction of drop sizes for liquid-liquid systems in stirred slim reactors - Part II: Multiple stage impellers. *Chem. Eng. J.* 2011, *168*, 827–838.
[32] Wulkow, M., Gerstlauer, A., Nieken, U., Modeling and simulation of crystallization processes using parsival. *Chem. Eng. Sci.* 2001, *56*, 2575-2588.
[33] Raikar, N. B., Bhatia, S. R., Malone, M. F., Henson, M. A., Experimental studies and population balance equation models for breakage prediction of emulsion drop size distributions. *Chem. Eng. Sci.* 2009, *64*, 2433-2447.
[34] Maaß, S., Kraume, M., Determination of breakage rates with single drop experiments. *Chem. Eng. Sci.* 2011, pp. 20.
[35] Kunst, B., Mencer, H., On Initial Drop Size Distribution in Mechanically Prepared O/W-Emulsions. *Kolloid Z. Z. Polym.* 1968, *228*, 77-78.